Chapter 3

MATERIALS AND METHODOLOGY

This chapter deals with the experimental procedure used in conducting the investigation for the development of titanium alloy and characterization for microstructural, mechanical, corrosion, wear, and in-vitro biocompatibility properties.

3.1. Material selection for the development of ternary titanium alloy

In the present study, the powder of titanium, copper, and niobium is purchased from Alfa Aesar (U.K.) of mesh size 325 (44 μm), having a purity of 99.96%. The BT-XRD test is carried out for confirmation of purity. Table 3.1 shows the details about the property of the powder used in this study.

Table 3.1. Purity and supplier of the purchased powder

S. No.	Materials	Initial purity	Supplier	Physical state
1	Ti	99.99%	Alfa Aesar, UK	Powder
2	Cu	99.99%	Alfa Aesar, UK	Powder
3	Nb	99.99%	Alfa Aesar, UK	Powder

3.2. Development of ternary titanium alloy

The powder metallurgy technique is used for the development of titanium alloy. Metal powder of the desired weight ratio was ball milled in RETSCH PM 400 planetary ball mill using a tungsten carbide jar and 10 mm diameter tungsten carbide ball (ball to powder ratio 10:1) in an inert atmosphere (argon ≥ 99.99% purity) to avoid oxidation. To prevent the sticking of metal powder in the periphery of the jar and ball, milling was done for 5 h at the speed of 200 rpm in the presence of toluene. After it, the alloy powder was uniaxially compressed by the manual press in tool steel die of 15 mm diameter at 650 MPa for 30 s. All samples were then kept in a

high vacuum (10^{-6} torr) quartz tube sealed on both sides and sintered at 900 ˚C in an inert atmosphere for 1 h with a heating rate of 5 ˚C min^{-1}. After the sintering, the samples were cooled down in the furnace to room temperature. The schematic diagram of the ball milling process and compaction of powder is shown in Fig. 3.1 and 3.2.

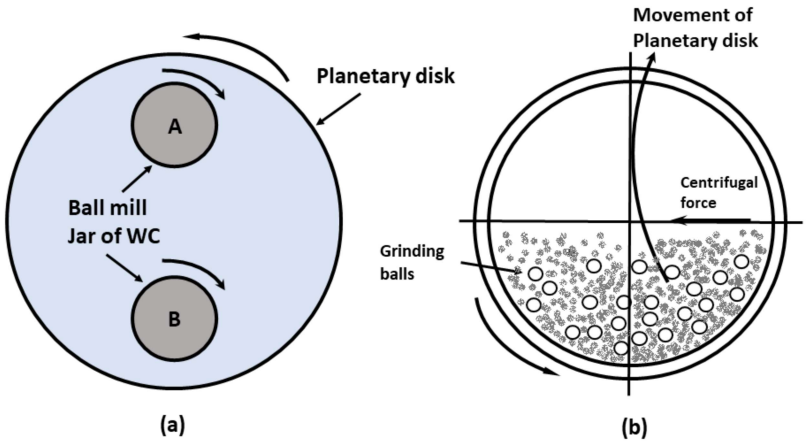

Fig. 3.1- The schematic diagram of the ball milling process

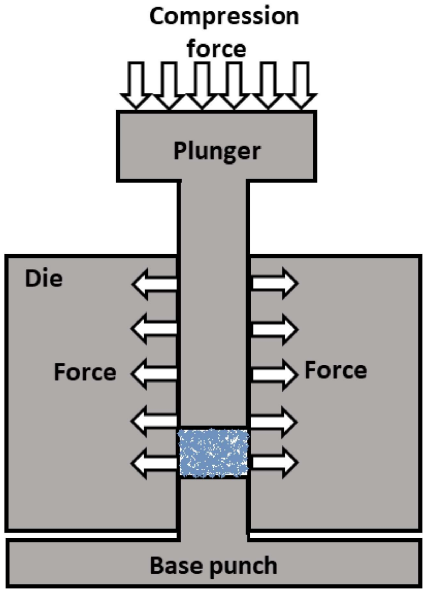

Fig. 3.2- The schematic diagram of compaction of powder in die.

The flow chart of the processing technique is also shown below in Fig. 3.3. After the furnace cooling; the samples were taken by breaking the tube. The pictorial image of the alloys after sintering is shown in Fig. 3.4.

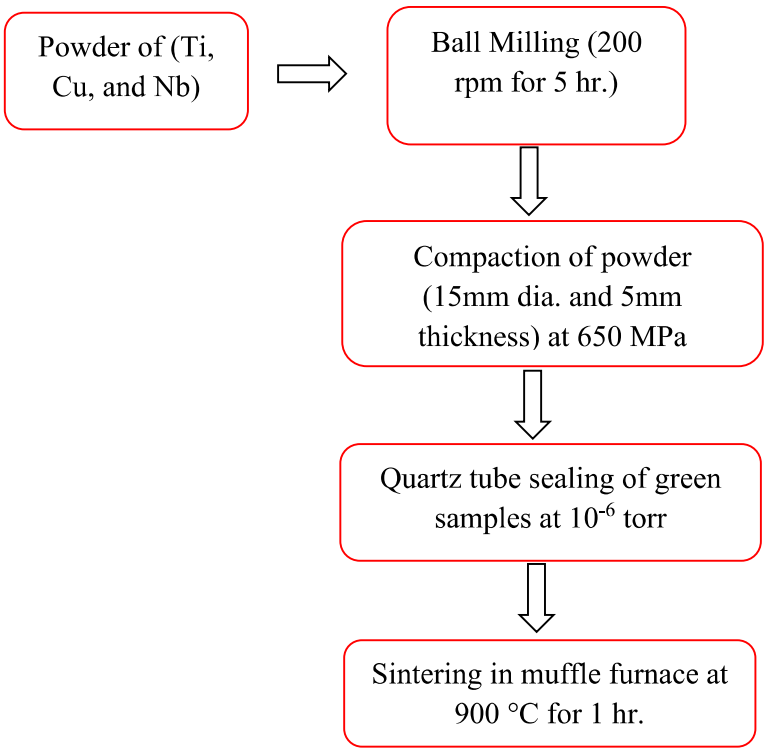

Fig. 3.3- The process flow chart of the development of ternary titanium alloy

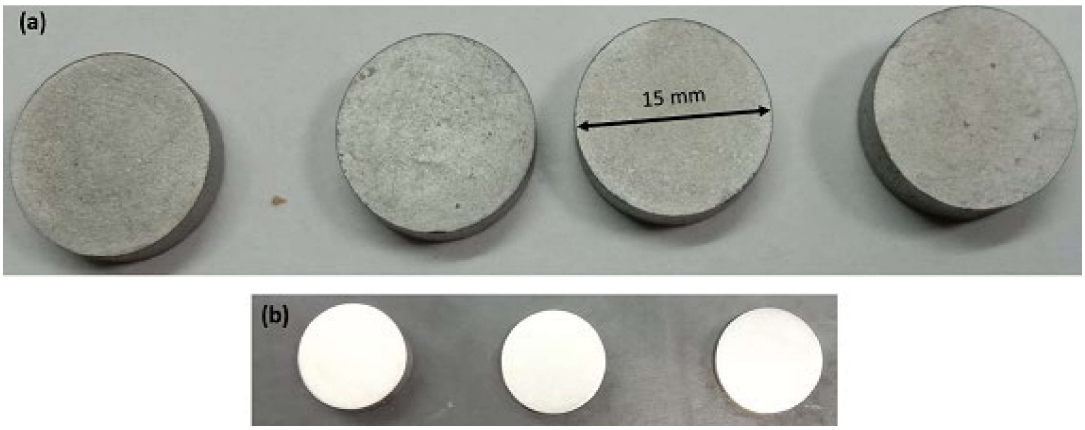

Fig. 3.4 - The pictorial image of the alloy (a) after sintering and (b) after cloth polishing

The sintered titanium alloys were named S1 (Ti-5Cu), S2 (Ti-5Cu-5Nb), S3 (Ti-5Cu-10Nb), and S4 (Ti-5Cy-15Nb) for convenience in writing. The composition and nomenclature of the sintered alloys are listed in Table 3.2.

Table 3.2. The nomenclature and composition of sintered alloy

Alloy	Composition (wt.%)	Nomenclature
Ti-5Cu	Ti- 95%, Cu-5%	S1
Ti-5Cu-5Nb	Ti- 90%, Cu-5%, Nb-5%	S2
Ti-5Cu-10Nb	Ti- 85%, Cu-5%, Nb-10%	S3
Ti-5Cu-15Nb	Ti- 80%, Cu-5%, Nb-15%	S4

3.3. Phase Evaluation and Microstructural Characterizations

3.3.1 X-ray diffraction analysis of hybrid composites

X-ray diffraction investigation was carried out on samples of both milled powder and sintered alloy to find the lattice strain, crystalline size, and phase present. X-ray diffraction (XRD) was performed by Rigaku Desktop Miniflex II X-ray diffractometer (Tokyo, Japan) with Ni-filtered Cu-Kα emission (λ= 1.5406Å) operated at 40KV/30 mA with a scanning speed of 5°/min in the angle (2θ) range between 20-90°. For all the intensity peaks and corresponding value of 2θ, the inter planer spacing, d, was evaluated using Bragg's law given by Eq. 3.1, which is ultimately utilized for the detection of different phases with the help of X-ray diffraction statistics details (JCPDS).

$$2d \sin\theta = n\lambda \tag{3.1}$$

where, θ – Incident angle

λ- wavelength of X-ray

n- an integer representing the order of the diffraction.

The lattice strain and crystalline size were evaluated by the Scherrer calculator inbuilt option in Xpert-Highscore data analysis software. The volume fraction of the formed phases after the sintering of all the alloys was calculated using equation 3.2.

$$W_p = \frac{P}{\sum P_i} \times 100 \tag{3.2}$$

Where P= relative intensity of phase p and $\sum P_i$ = The sum of the relative intensity of all observed phases.

3.3.2 Microstructural characterization

For microstructural characterization, samples were manually polished following the standard metallographic procedure, as discussed below. The surface of the sample that is to be examined was first made plane by silicon carbide emery paper (Buehler, USA) of different grit (200, 320, 400, 600, 800, 1000, 1200, 1500, 2000, and 2500) one by one. During polishing on each emery paper, the samples were kept vertically and moved in either direction. After examining the surface of the sample, the final cloth polishing was completed using velvet cloth with 0.9 µm diamond paste and spray (Chennai Metco) on an automatic polishing machine (Banipol, Metco, Chennai, India). After polishing, the samples were ultrasonically cleaned in ethanol for 10 min and finally dried in hot air. Finally, when the scratches were removed from the surface, the sample was examined using an optical microscope (OM, Leica Z6 APO).

After this, the microstructural study of all the samples was also examined by high resolution scanning electron microscope (HR-SEM) equipped with energy dispersive analysis of X-ray (EDAX) to explore the compositional analysis (Model No. NOVA NANO SEM 450). HR-SEM helps to a better understanding of the phases formed after the sintering at high resolution. The elemental mapping of samples was also shown by the HR-SEM. These optical, HR-SEM microstructure, EDAX spectrum, and elemental mapping of the sintered alloy are presented and discussed in Chapter 4.

3.4 Mechanical properties testing

3.4.1 Density measurement of sintered alloy

The density of the alloy after sintering is measured using Archimedes' principle (ASTM C 693) with the help of the calculated weight of the alloy both in air and water using an electronic weight balance with an accuracy of 0.0001g. The theoretical density of the alloy is calculated

using the rule of the mixture of alloy. The relative density and porosity of the alloy are calculated by using equations 3.3 and 3.4, respectively.

$$Relative\ density(\%) = \left[\frac{sintered\ density}{theorectical\ density}\right] \times 100 \quad (3.3)$$

$$Porosity(\%) = \left(1 - \frac{\rho_s}{\rho_t}\right) \times 100 \quad (3.4)$$

Where ρ_s is the density of sintered alloy and ρ_t is the theoretical density of the alloys.

3.4.2 Micro-hardness measurements

The hardness test is one of the significant mechanical tests for evaluating the property of the materials used in structural analysis, engineering design, and development of materials. The hardness of any material is resistance against permanent deformation such as scratches, wear, indentation, and abrasion. Hardness testing is more significant in establishing the correlation between hardness and other's material properties.

The Vicker hardness test is used to evaluate the hardness of the sintered alloy. The Vickers method is based on an optical measurement system. The Microhardness test procedure, ASTM E-384, specifies a range of light loads using a diamond indenter to make an indentation which is measured and converted to a hardness value. The micro-hardness values of all the sintered samples were obtained using a Microhardness tester (LECO: LV 248AT) with a 0.5 kgf load and a 10 s dwell period. Ten indentation readings on each sample were taken at different positions, and the mean value ± standard deviation was calculated as the hardness value. The Vickers indentations and their corresponding diagonal measurements are shown in Fig. 3.5 (a) and (b), respectively. The Vickers microhardness machine has a diamond indentor shaped like a pyramid with a square base and a 136-degree angle between the two sides. The specimen is subjected to loads ranging from 1gf to 100 kgf. The dwell duration used for the test is typically 10 to 15 seconds. A microscope is used to view the indentation impression left on the test specimen when the load is applied and to calculate the average of the two diagonals of the indentation left on the specimen's surface after the load has been removed. Calculations are

made to determine the area of the indentation's sloping surfaces. The relationship between the applied load and the square mm area of the indentation determines the Vickers hardness. The indentation impression is seen on the test when the load is applied.

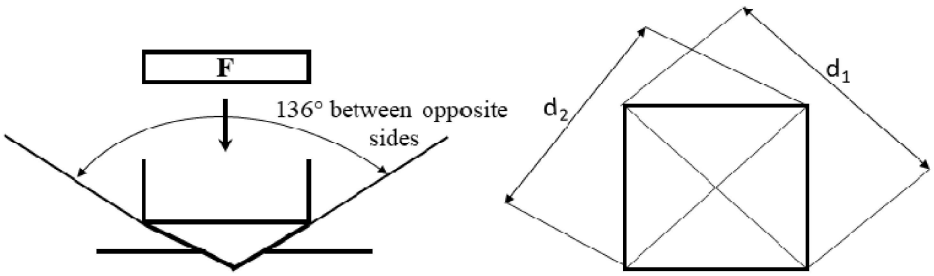

Fig. 3.5- (a) indentation marked by indenter and (b) measurements of diagonal dimension

The Vickers microhardness is calculated by using the formula:

$$HV = \frac{2P\ sin\frac{\theta}{2}}{D^2} \tag{3.5}$$

Where P = load applied (kgf)

D = mean diagonal of the indentation (mm)

θ = angle between opposite faces of the diamond = 136°

It is very useful for testing on a wide type of materials, but test samples must be highly polished to enable measuring the size of the impressions.

3.4.3 Compression test

The compressive strength of any material is checked to understand the resisting capability of the material under compression load. The lower compressive strength of the load-bearing biomaterial also caused the early failure of the implant. The compression test of all four sintered titanium alloys was tested according to ASTM E9-09 on the universal testing machine (INSTRON 5982). The length and diameter of the samples were 12 mm and 6 mm (cut by wire electric discharge machining from Φ15 mm × 8 mm thick sample), respectively (L/D = 2.0), with the cross-head velocity of 0.5 mm/min under a load capacity of 100 kN. The end surface

of the sample was maintained normal to the axis of the specimen. Figure 3.6 shows the compression test setup during the test.

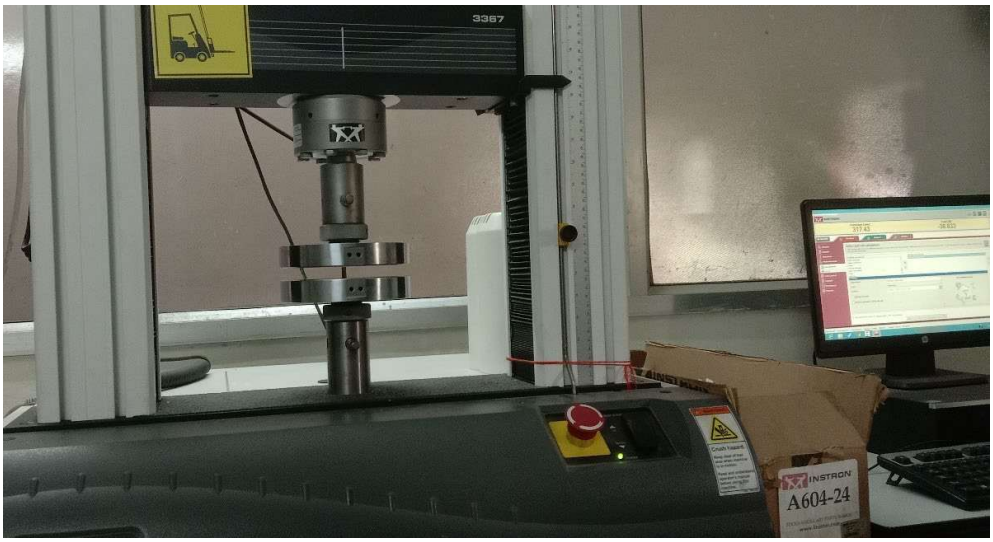

Fig. 3.6- Pictorial image of the INSTRON universal testing machine during the compression test

3.5 Electrochemical corrosion measurements

According to the theory of electrochemical corrosion, corrosion happens as a result of electrochemical processes, such as an anodic reaction, also known as an oxidation reaction, and a cathodic reaction, also known as a reduction reaction. Corrosion is a chemical degradation caused by the surrounding fluid. The bio-implant is always in contact with the surrounding fluid. The in-vitro chemical corrosion behavior of the sintered alloys was conducted using the electrochemical polarisation technique. The sintered alloys were evaluated for corrosion performance in a simulated body fluid (SBF) (pH=7.4) at room temperature. The image of the potentiostat during the testing is given in fig. 3.7, and the composition of the simulated body fluid is listed in Table 3.3.

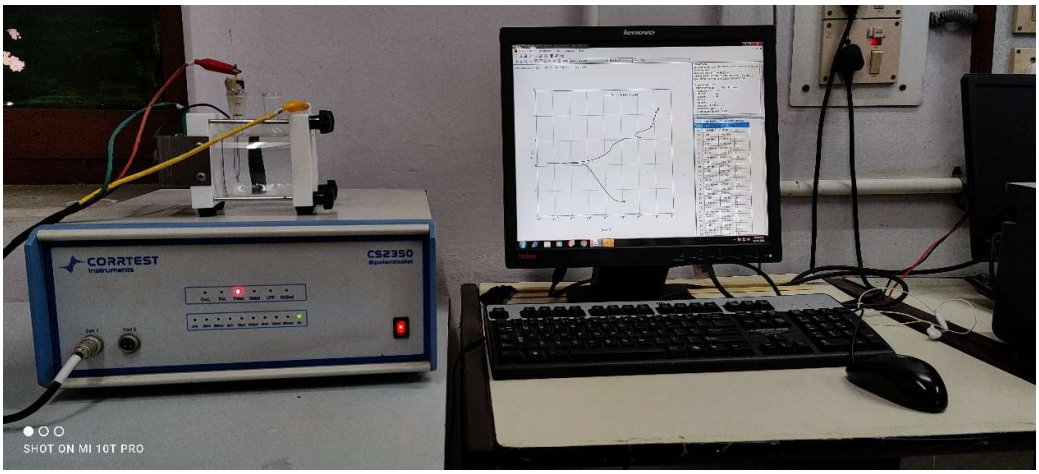

Fig. 3.7- Image of the CCORRTEST CS 2350 Potentiostat test setup during testing

Table 3.3- Chemical composition of the reagents in 1000 mL simulated body fluid

Reagents	**Amount in 1000 mL**
NaCl	8.035 g
$NaHCO_3$	0.355 g
KCl	0.225 g
$MgCl_2.6H_2O$	0.311 g
Na_2SO_4	0.072 g
1.0M HCl	39 mL
$CaCl_2$	0.292 g
$((HOCH_2)_3CNH_2)$	6.118 g

The open-circuit potential (OCP), electrochemical impedance spectroscopy (EIS), and potentiodynamic polarization measurement techniques were used to investigate the sintered alloy's corrosion behavior. The electrochemical quantities were carried out in a glass cell at room temperature consisting of a three-electrode cell, which was linked to a potentiostat controlled by a computer (CORRTEST Instruments CS2350 Bi-Potentiostat, China). The uncovered surface (1 cm^2) of the samples served as the working electrode in corrosion experiments utilizing the usual three-electrode cell technique [saturated Ag/AgCl as the

reference electrode, Platinum sheet as the counter-electrode]. In SBF, the OCP of each alloy was measured continuously for 3600 seconds. After the OCP measurements, the EIS test was conducted using an A.C. amplitude range of -10 mV to +10 mV and a frequency range of 10^{-2} Hz to 10^{+5} Hz. Using the extrapolation method, the EIS data were explained in Nyquist and Bode-phase plots. After the EIS test, a scan rate of 1 mV per second was used to estimate the potentiodynamic polarisation with an initial potential of -1.6 V to +2.1 V from OCP. Tafel analysis based on the polarisation plots estimates corrosion parameters such as corrosion potential (E_{corr}) and corrosion current density (i_{corr}), passive current density (i_{pp}), and breakdown potential from the polarisation plots. Three parallel samples were used for each group in the experiments to achieve repeatability. After the potentiodynamic polarization test, the surface of the samples is examined by SEM and XPS tests to examine the formation of the titanium, copper, and niobium oxide.

3.6 Wear test of the sintered alloys

The reciprocating wear and friction test of the sintered alloys were tested in an automated Ducom Bio- tribometer (Bengaluru, India) under wet conditions (fig. 3.8). In the tests, the samples acted as the stationary body, whereas the moving body was the counter material. They were performed under lubricated conditions with varying loads to compare different conditions since they have an essential role in the tribological properties of materials. Sintered alloys (ϕ 15 mm and 4 mm thickness) as a disc and a ZrO_2 ball of 10 mm diameter as counter material were taken for the study. The reciprocating wear track was 5mm. The normal load of 10, 15, and 20N was applied to the counter material. The frequency of 2 Hz for 3600 cycles on a 5 mm sliding distance in the presence of SBF was used for all the tests. The length of the wear track was taken as 5 mm (stroke length). The schematic diagram of the wear test is shown in fig. 3.9. The width and the lateral depth of the wear track were measured by a contact profilometer (Taylor and Hobson, England).

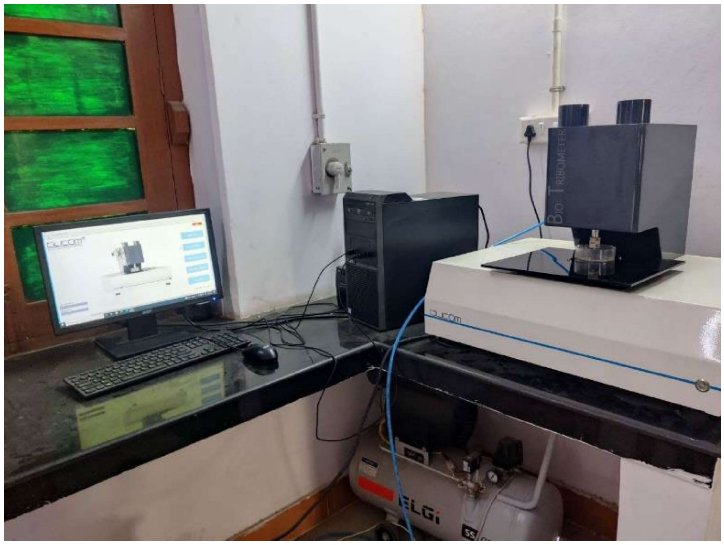

Fig. 3.8- Image of the Tribometer used for wear study.

The wear loss of the worn profile was first measured using a profilometer to calculate the wear loss volume. The average depth values were then calculated using the following formula (Doni et al., 2013):

$$D_{avg} = \frac{A_w}{W} \tag{3.6}$$

where D_{avg} , A_w , and W is the average depth in mm, average wear loss area, and the average width of each worn track, respectively, measured by a profilometer. Finally, wear volume loss was intended with the following formula:

$$\Delta V = \left[\frac{1}{3} * \pi * D_{avg}^2\left(3R - D_{avg}\right)\right] + A_w * l \tag{3.7}$$

where ΔV, R, and l are the volume loss (mm^3), the radius of the zirconia ball (mm), and the length of the wear track (5 mm) for each wear track, respectively. The following formula has been used to generate the volume loss values into wear rate:

$$W_v = \frac{\Delta V}{S} \tag{3.8}$$

where, W_v denotes the wear rate in mm^3/mm, ΔV is the volume loss in mm^3, and S denotes the overall sliding distance in millimeters.

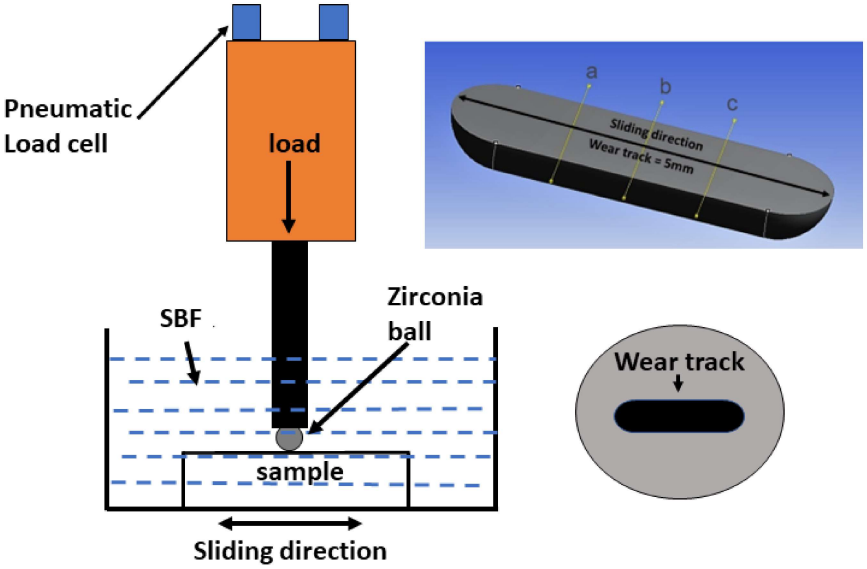

Fig. 3.9- schematic of tribological study in reciprocating linear motion of samples in SBF.

All experiments were repeated at least three times to achieve repeatability. The wear rates were calculated using three tracks per condition. After the wear test, the sample was ultrasonically cleaned in ethanol for ten min.; then, worn surface analysis was done using the 3D surface profilometer (Taylor Hobson, UK), Field emission scanning electron microscopy (FE-SEM, Nova Nano SEM 450) equipped with Energy Dispersive X-ray Spectroscopy (EDS), and scanning probe microscope (SPM, NTEGRA Prima).

3.7 Cell culture and antibacterial test

3.7.1 Cell Study:

The cytocompatibility of samples has been evaluated using MG-63 cells. The MG-63 (human osteosarcoma) cells were procured from (NCCS Pune, Maharashtra, India). The DMEM media (Dulbecco's modified eagle medium) with 15 % fetal bovine serum (FBS) and 1 % antibiotics were used as culture medium. The cells (Cell density: 10^4 cells/ml) were seeded onto the samples kept in 24 well plates and incubated in standard atmosphere (37 °C, 5 % CO_2, and

95% relative humidity) for cell growth to investigate the cellular response quantitatively (MTT assay) and qualitatively (fluorescence microscopy). A change of the DMEM medium was made after every 48 or 72 hours.

3.7.3 Cell proliferation

Cell growth on biomaterials is generally accessed using MTT [3-(4, 5-dimethylthiazol-2-yl)-2, 5-diphenyl-tetrazolium-bromide] test. After 3, 5, and 7 days of cell culture on samples were evaluated. As a control sample, glass cover slips were used. Each sample had its culture removed after incubation, and then it was rinsed twice with 1x PBS (phosphate buffer saline) solution. Again, the samples were incubated for 6 hours in a prescribed atmosphere to allow the reaction of the reconstituted MTT with the live cells to produce formazan crystals. After six hours, dimethyl sulfoxide (DMSO) was added to the MTT solution in each well, and the wells were once more incubated for ten minutes in the same environment to dissolve the formazan crystals. The quantity of these formazan crystals corresponds to the viability of live cells, which was assessed using an ELISA Microplate (iMark Bio-red) reader to detect optical density at 595 nm.

3.7.4 Morphological analysis:

Fluorescence microscopy was used to examine how MG-63 cells adhered to and changed in shape when placed on samples. After three days of incubation, the adherent cells were fixed with paraformaldehyde (4 %) for 30 minutes at 4 °C. After that; the cells were permeabilized with Triton X-100 (0.1%) for 10 minutes at room temperature. Now, bovine serum albumin was added to block these permeable cells. Alexafluor 488 Phalloidin and DAPI dyes were used to stain the MG63 cells' nucleus and cytoskeleton, respectively. With the use of a fluorescent microscope (Nikon Eclipse LV 100 ND), the cells were imaged.

3.7.5 Antibacterial test

3.7.5.1 Preparation

The antibacterial test of all the sintered alloy was performed in the microbiology laboratory of the Institute of Medical Science, Banaras Hindu University. About 10.0 g peptone, 5.0 g beef extract, 5.0 g NaCl, and 15.0 g agar were dissolved in 1 l distilled water to prepare nutrient broth (NB), and the pH level was kept between 7.3 and 7.4. The pH of the phosphate buffer saline (PBS) solution was adjusted to 7.2–7.4 after dissolving 2.83 g Na_2HPO_4 and 1.36 g KH_2PO_4 in 1 L distilled water. The NB and PBS solutions were autoclaved for 20 min at 121 °C to sterilize them. The strains employed in this investigation were S. aureus ATCC 6538 and E. coli ATCC 25 922. The bacteria were grown to a concentration of 10^6 CFU ml^{-1} in nutritional broth at 37 °C, then diluted ten times in PBS solution to 10^4 CFU ml^{-1} (bacterial suspension). Before starting the experiment, UV irradiation was used to sterilize all glassware and samples.

3.7.5.2 Plate count method

The plate count method was carried out according to the National Standard of China GB/T 2591 (JIS Z 2801-2000, ASTM G21-96, NEQ). Both the samples and the control sample (CP-Ti) were rested in separate Petri dishes. Nutrient agar was put onto a Petri dish as a negative blank sample. After this, 0.4 ml of the bacterial suspension was poured on all these samples, including the control sample, test sample, and negative sample. Then, the dishes were covered with a relatively large Petri dish and put for incubation for 24 h under a humidity of 90% at the temperature of 37 °C. After incubation, the contaminated strain was washed in 3.6 ml of sterile physiological saline solution and transferred to a sterilized Petri dish. The samples were thoroughly cleaned to ensure that no bacteria remained on them. About 0.02 ml of the above-mentioned washing solution was inoculated into nutrient agar plates and incubated for 4 h with a humidity of 90% at the temperature of 37 °C. After this, the number of colonies of the bacteria

was counted. Three samples of each alloy were inspected for repeatability. The antibacterial rate (R) was obtained using the following formula:

$$R = \frac{N_{control} - N_{sample}}{N_{control}} \times 100\% \quad (3.9)$$

where, N_{sample} and $N_{control}$ are the numbers of the bacterial colony on the sintered alloy S1, S2, S3, and S4, and the control sample, respectively.